SPRAY 2012
10. Workshop über Sprays, Techniken der Fluidzerstäubung und Untersuchung von Sprühvorgängen
Berlin 21.-22. Mai 2012

Numerical simulation of monodisperse droplet generation in nozzles

O. Mierka, H. Damanik and S. Turek

Institute of Applied Mathematics (LS III), TU Dortmund
Vogelpothsweg 87, D-44227, Dortmund, Germany

omierka@math.tu-dortmund.de, hdamanik@math.tu-dortmund.de,
stefan.turek@math.tu-dortmund.de

Abstract

In this contribution further development of our in-house FEM based parallel 3D simulation tool FeatFlow will be presented. In particular, we give an insight into the recent developments of the Level Set based multiphase module, which has been extended with high order (Q_2) discretization to increase the robustness and accuracy of the arising prediction tool for the simulation of monodisperse droplet generation processes. According to the given extension, an implementation of the surface reconstruction has been performed which on one hand guarantees the exact identification of the interface and on the other hand offers the advantages of the underlying multilevel structures to perform octree fashioned highly efficient reinitialization of the Level Set field.

Validation of the newly extended 3D simulation tool was performed on the well established two dimensional benchmark configuration involving the rising bubble problem. Results of numerical simulations for more realistic gas-liquid systems are to be presented and compared with three dimensional experimental and computational reference results.

Further extension of the developed simulation tool with non-Newtonian rheological (shear rate dependent viscosity) models has been realized and validated on the "flow around cylinder" benchmark problem. Subsequently, investigations in terms of numerical simulations for the rising bubble configurations have been performed and compared to reference data.

Finally, results of numerical simulations involving droplet generation from a nozzle are to be presented and further application of the developed simulation tool is discussed.

1. INTRODUCTION

Multiphase flow problems are very important in many applications, and performing accurate, robust and efficient numerical simulations of them has been the object of numerous research and simulation projects for many years. One of the main challenges for the underlying numerical merhods is that the position of the moving interface between two fluids is unknown and part of the boundary value problem which should be solved. If we assume a domain Ω with two immiscible fluids, then the time dependent subdomains $\Omega_1(t)$ and $\Omega_2(t)$ are bounded by an external boundary Σ and a dynamic interior boundary or interface $\Gamma(t)$ which might consist of several components.

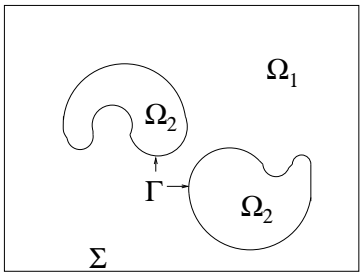

Complete domain Ω.

The usual model for laminar fluids is described by the incompressible Navier-Stokes equations

$$\rho(\mathbf{x})\left[\frac{\partial \mathbf{u}}{\partial t} + \mathbf{u}\cdot\nabla\mathbf{u}\right] - \nabla\cdot(\mu(\mathbf{x})[\nabla\mathbf{u} + (\nabla\mathbf{u})^T]) + \nabla p = \rho(\mathbf{x})\mathbf{g} + \mathbf{f}_\Gamma(\sigma), \tag{1}$$

$$\nabla\cdot\mathbf{u} = 0 \qquad \text{in} \qquad \Omega = \Omega_1 \cup \Gamma \cup \Omega_2, \tag{2}$$

which contain an additional force term $\mathbf{f}_\Gamma(\sigma)$ due to the surface tension σ at the free interface Γ. Here, the density ρ as well as the viscosity μ are discontinuous and depending on the interface location $\Gamma(t)$, that is

$$\rho(\mathbf{x},t) = \begin{cases} \rho_1, & \forall\ \mathbf{x} \in \Omega_1(t) \\ \rho_2, & \forall\ \mathbf{x} \in \Omega_2(t) \end{cases}, \qquad \mu(\mathbf{x},t) = \begin{cases} \mu_1, & \forall\ \mathbf{x} \in \Omega_1(t) \\ \mu_2, & \forall\ \mathbf{x} \in \Omega_2(t) \end{cases} \tag{3}$$

which significantly influences the continuous velocity $\mathbf{u}$ as well as the pressure p.

This contribution describes the implementation and application of a new Level Set approach in the framework of the Finite Element Method (FEM). For this reason the open-source CFD package FeatFlow was utilized and was newly extended with the corresponding high order Level Set module. The main advantages of the developed CFD package are as follows:

- Parallelization based on domain decomposition
- High order FEM discretization schemes in space and time
- Use of 3D unstructured meshes
- Highly efficient Newton-Multigrid solvers
- Accurate surface reconstruction technique
- Robust reinitialization procedure

The discretization of the arising equations in space is performed by an unstructured grid finite element method. The incompressible Navier-Stokes equations are discretized using the Q_2/P_1 element pair, whereas high order Q_2 elements are employed for the discretization of the Level Set equation. After an implicit time discretization by the Crank-Nicolson method the Navier Stokes and Level Set advection equations are solved in an operator splitting approach via the Discrete Projection Method [7, 8].
In the following sections we give an insight into the description of the mathematical framework of the Newtonian/non-Newtonian Navier Stokes equations within the multiphase environment and into the recent development of our Level Set based methodology. In the numerical sections we concentrate on the validation of our newly redesigned CFD tool for the well established "Rising bubble problem" [5] and then give an insight into our prototypical development in 2D viscoelastic multiphase flow simulations. The numerical simulations section continues with the discussion on 3D droplet dripping results and the study is closed by our conclusions and future visions.

2. MATHEMATICAL MODEL

2..1. Description of the Level Set module

In the current work the location of the free interface Γ is captured by means of the Level Set approach which represents the interface as a zero isosurface of a continuous indicator function ϕ and its distribution in the complete domain Ω can then be calculated via the following scalar transport equation:

$$\frac{\partial \phi}{\partial t} + \mathbf{u} \cdot \nabla \phi = 0 \tag{4}$$

Since ϕ approximates a distance function it is smooth and it allows the calculation of the globally defined normal vector $\mathbf{n}$ towards the interface Γ and of the corresponding curvature via

$$\mathbf{n} = \frac{\nabla \phi}{|\nabla \phi|}, \qquad \kappa = -\nabla \cdot \mathbf{n} = -\nabla \cdot \left(\frac{\nabla \phi}{|\nabla \phi|} \right). \tag{5}$$

Here, special FEM techniques for gradient recovery can be used which allow highly accurate approximations of normals and curvature which are necessary for the direct evaluation of the surface tension force $\mathbf{f}_\Gamma = \kappa\sigma\delta(\phi)\mathbf{n}$, with $\delta(\phi)$ denoting the corresponding Dirac Delta function.

Development and implementation of a typical Level Set approach consists of performing the following sequence of tasks:

- Advection of the Level Set field on the underlying velocity field $\mathbf{u}$ (4).
- Reinitialization of the Level Set field
- Recovery of the normal vector $\mathbf{n}$ and curvature κ fields
- Evaluation of the discontinous fluid parameters ρ, μ, and $\mathbf{f}_\Gamma$ based on the reconstructed distribution of Γ.

One has to keep in mind that the reinitialization of the Level Set field is nececcary for two main reasons, and these are that by reinitialization the Level Set field becomes smooth and stabilization of the convection terms does not need to be incorporated, while the second reason is that the recovery of the curvature (5) requires as an input an exact distance field. On the other hand, it is well known from the literature, that the reinitialization of the Level Set field leads to artificial "movement" of the interface, and may exhibit even its systematic translation in cases when it is performed too often. That is the reason why the two previously mentioned requirements can be satisfied through an additionally introduced field, $\tilde{\phi}$. According to the proposed approach one can reinitialize the Level Set field ϕ into $\tilde{\phi}$ and all the postprocessing steps (recovery of the normals, curvature and physical properties) are then performed only with respect to $\tilde{\phi}$ (which is the most accurate approximation of the distance distribution) without influencing the interface. This way, reinitialization of the Level Set field ϕ becomes crucial only for stability reasons. The link between the fields ϕ and $\tilde{\phi}$ is the interface Γ which is reconstructed from the Level Set distribution ϕ at every timestep. During this global surface reconstruction process all elements of the computational domain intersected by the interface are visited and according to the used high order Q_2 element the zero level surface is triangulated in a recursive fashion so to provide subgrid resolution of the interface. A complete set of triangles of a reconstructed surface immersed into the computational hexahedral mesh for a droplet dripping simulation is illustrated in Fig. 1. The arising set of triangles is then organized into groups with respect to the elements they originate from. Due to the underlying multigrid mesh structure this data management is performed in a hierarchical manner while for the coarser level representation for efficiency reasons only the mass of points of the individual groups are to be used. This allows us to design a very efficient reinitialization algorithm, which starts on the coarse representation of the surface and ends by determination of the closest triangle to an analyzed point. The role of efficiency in such a "point to triangle distance" implementation plays a crucial role since the reinitialization offered by us is related to an L_2 projection, as follows:

$$\int \tilde{\phi} w \, dx = \int \text{dist } w \, dx, \tag{6}$$

where w is the Q_2 basis funcion and dist is the distance which on the level of practical realization means the evaluation of the distance with respect to the surface in each cubature point during the numerical integration. This linear equation can be also solved iteratively by the help of the lumped mass matrix M_L, and according to our experience even the first iteration of this solution process provides an accurate approximation:

$$\tilde{\phi} = M_L^{-1} \int \text{dist } w \, dx. \tag{7}$$

Then, for the reinitialization of the Level Set function two procedures offer themselves. The first alternative is a full one ($\phi := \tilde{\phi}$) with a given frequency f_{reini} or according to the second alternative it can be performed in an underrelaxation sense even at every timestep:

$$\phi := M_L^{-1} \int (\alpha_{\text{reini}} \text{dist} + (1 - \alpha_{\text{reini}})\phi)\, w\, dx. \tag{8}$$

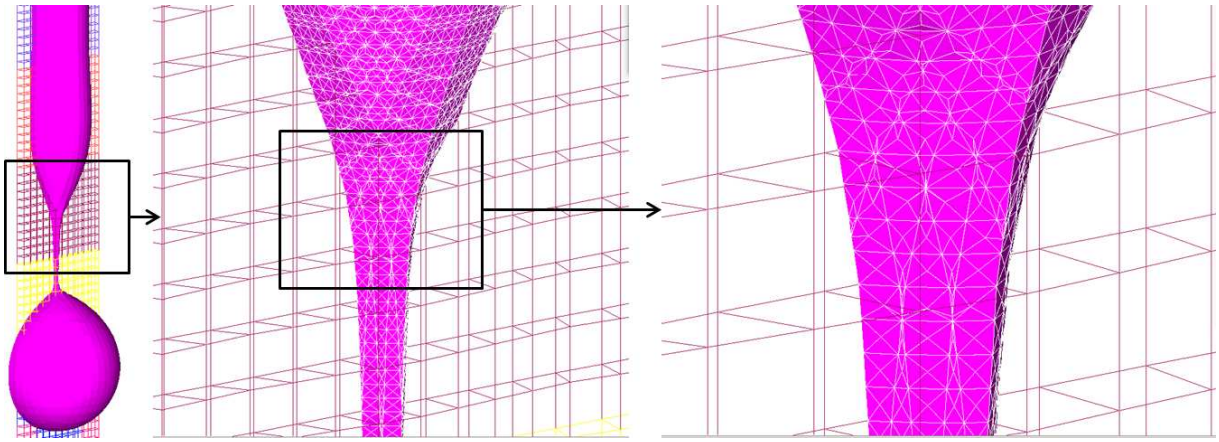

Figure 1: Illustration of a triangulated surface reconstruction.

2..2. Description of the Non-Newtonian module

Fluid 1 is a viscoelastic fluid described by the Oldroyd-B model based on the conformation tensor τ

$$\frac{\partial \tau}{\partial t} + (\mathbf{u} \cdot \nabla)\tau - \tau \cdot \nabla \mathbf{u}^T + \frac{1}{\Lambda}(\tau - \mathbf{I}) = 0. \tag{9}$$

Fluid 2 is a liquid bubble given by a Newtonian model, $\tau_s = 2\eta_s(\mathbf{x}, t)\mathbf{D}$, with viscosity $\eta_s(\mathbf{x}, t)$ in each fluid phase. Here, $\mathbf{D} = \frac{1}{2}(\nabla \mathbf{u} + \nabla \mathbf{u}^{\mathrm{T}})$ is the deformation tensor. Both fluids are governed by the Navier-Stokes flow equations, i.e.

$$\rho(\mathbf{x}) \left[\frac{\partial \mathbf{u}}{\partial t} + \mathbf{u} \cdot \nabla \mathbf{u} \right] = \nabla \cdot \mathbf{T} + \rho(\mathbf{x})\mathbf{g} + \mathbf{f}_\Gamma(\sigma), \tag{10}$$

$$\nabla \cdot \mathbf{u} = 0 \qquad \text{in} \qquad \Omega = \Omega_1 \cup \Gamma \cup \Omega_2, \tag{11}$$

where the density depends on the position. The hydrostatic pressure p, the viscous- and the elastic-tensor contribute to the total stress tensor so that we can write

$$\mathbf{T} = -p\mathbf{I} + \tau_s + \frac{\eta_p(\mathbf{x})}{\Lambda}(\tau - \mathbf{I}). \tag{12}$$

The above listed system of strongly coupled equations (9)–(12) is solved in a monolithic fashion with the reformulation of (9) in the "LCR" sense [2] and with the support of robust Newton-multigrid solvers [3].

3. NUMERICAL SIMULATIONS

3..1. 2D Rising bubble in Newtonian fluids

According to the benchmark configuration introduced by Hysing *et al.* [5] both 2D test cases were simulated with our newly redesigned multiphase code in 3D so that free slip boundary conditions were imposed on the front and back wall of the rectangular (1 x 2) domain so that only one layer of element on the coarse grid was used to resolve the invariant third dimension.

The corresponding physical parameters for the two test cases are listed in Tab 3..1.. The first test case models a rising bubble with $Re = 35$, $Eo = 10$, which according to the experimental studies of Clift *et al.* [1] is predicted to happen in the ellipsoidal regime. The second and more challenging test case models a rising bubble with $Re = 35$, $Eo = 125$ and with ratios of physical properties of gas liquid systems. This bubble lies somewhere between the skirted and dimpled ellipsoidal cup regimes indicating that break up of the bubble is expected to happen.

Test case	ρ_1	ρ_2	μ_1	μ_2	$\mathbf{g}$	σ
1	1000	100	10	1	0.98	24.5
2	1000	1	10	0.1	0.98	1.96

The simulation results obtained for the simulation of the first benchmark problem are organized into Fig. 2, which shows the time evolution of the reference bubble shape at every 0.5 time units compared to our solution. In addition we give the detailed comparison of the final shape of the bubble (at $t = 3.0$) with respect to the reference solution. As it can be seen from the figures the solutions are almost not distinguishable even for the results obtained on the coarse grid (L1). It is also worth to mention that the mass loss during these simulations were also on a very low level (L1: 1.2%, L2: 0.7%, L3: 0.3%).

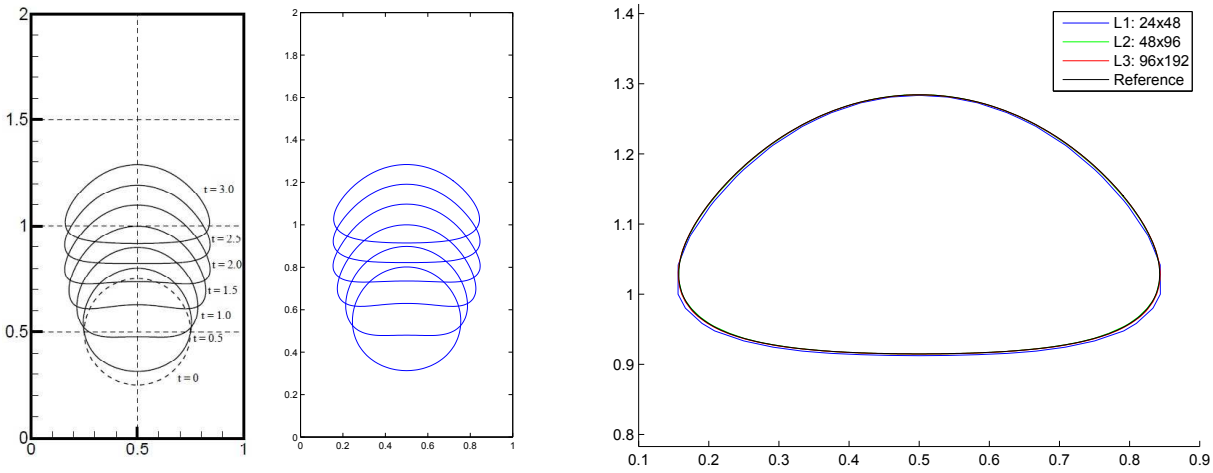

Figure 2: Case 1 bubble shapes for the rising bubble problem. Left and middle: Reference vs. our mesh independent result. Right: Mesh convergence for the final bubble shape vs. reference.

Since the second test case requires a very fine resolution due to the creation of thin filaments and satellite droplets even for a pure 2D simulation tool, with our 3D CFD code we were able to obtain mesh independent results only until time $t = 2.2$. On the other hand, one should also note that even the benchmark results from the three different groups [5] do not provide exactly the same results beyond this critical time. This is the reason, why we do compare (see Fig 3) with the reference values within this reduced time frame $t \in (0, 2.2)$ only.

3..2. 2D Rising bubble in viscoelastic fluids

There is no rigorous benchmark for a rising bubble in a viscoelastic liquid, but there exist numerical simulations for this purpose which tried to show a cusp shape as observed in the experimental results. The objective of the simulation is to obtain the cusp shape of the bubble and to compare the resulting rising bubble phenomenon with a bubble rise in a corresponding Newtonian fluid. The cusp formation is subject to certain conditions: The inertia effect (Re) must be small but the rising speed should be visible, the capillary number (Ca) should be bigger

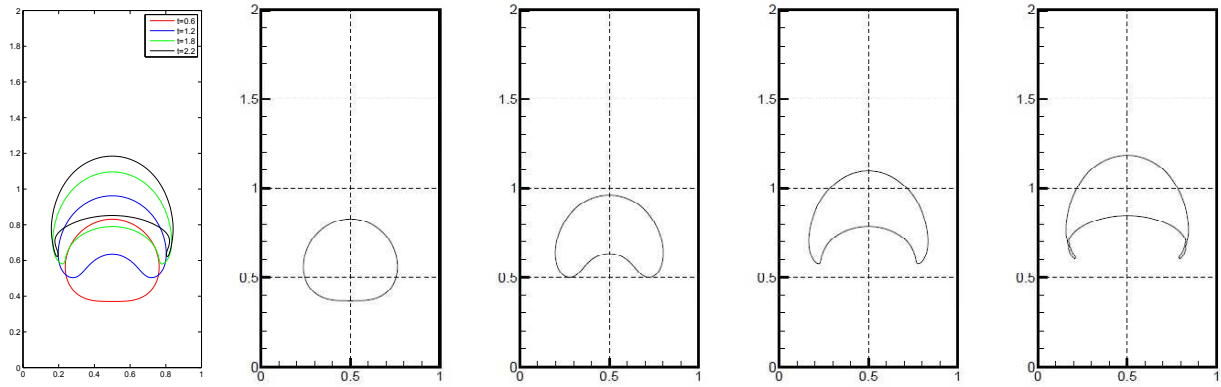

Figure 3: Case 2 bubble shapes for the rising bubble problem. Left: our results on mesh level 3 at times 0.6, 1.2, 1.8 and 2.2. The four others are the reference results at corresponding times.

than some critical number and the Weissenberg number does not vanish (We $\neq$ 0) [6]. The parameter settings for the following simulations are as follows:

Test case	ρ_1	ρ_2	μ_1	μ_2	$\mathbf{g}$	σ
1. Viscoelastic ($\Lambda = 10$)	10	0.1	10	1	9.8	0.245
2. Newtonian ($\Lambda = 0$)	10	0.1	10	1	9.8	0.245
3. Viscoelastic ($\Lambda = 10$)	10	0.1	2	1	9.8	0.245
4. Newtonian ($\Lambda = 0$)	10	0.1	2	1	9.8	0.245

On the other hand the geometrical configuration is kept the same as in the previous benchmark because the shape of the column does not influence the cusp formation [6] as long as it is aligned with the gravity (the column does not tilt). The first two test cases (Fig. 4) show a different rising bubble behaviour in viscoelastic and Newtonian surrounding fluids. The cusp starts to appear very late at numerical time $t = 5$. On the other hand, the last two test cases (Fig. 4)

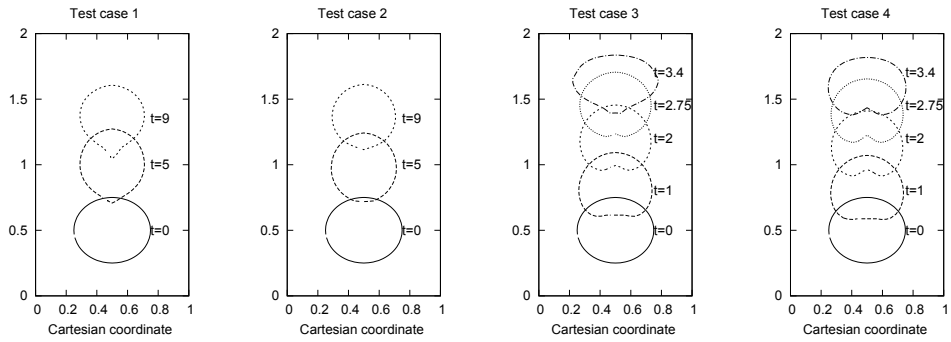

Figure 4: Evolution of bubbles for test cases 1-4

show that the bubble rises faster than the first two test cases because of more inertia. Already at time $t = 3.4$ the bubble is close to the upper wall which shows cusp formation. Since the numerical time is shorter than the first two test cases, mass loss is less visible here.

3..3. 3D Droplet dripping simulation

The experimental setup involved a two phase problem consisting of glucose-water mixture (as continuous phase) and silicon oil (as dispersed phase). The measurements were restricted to the so called dripping mode. This mode is characterized by relatively low volumetric flowrates and by the fact that the droplets are generated in the near vicinity of the capillary so that the

stream lenght is on the order of the generated droplets. Since the temperature was kept at a constant value during the whole experiment all physical properties of the present phases were constant. The experimental measurements were realized (by the group of Prof. Walzel, BCI, TU Dortmund) to obtain statistically averaged quantities such as droplet size, droplet generation frequency and stream length. These experimentally measured quantities were compared with our subsequent simulation results. The list of physical properties together with the geometrical parameters is as follows:

$$\rho_C = 1.34\ kg\ dm^{-3} \quad \rho_D = 0.97\ kg\ dm^{-3} \quad g_z = -98.1\ dm\ s^{-2} \quad \sigma = 0.034\ kg\ s^{-2}$$
$$\mu_{C,D} = 0.050\ kg\ dm\ s^{-1} \quad \dot{V}_C = 1.65\ 10^{-3}\ dm^3 s^{-1} \quad \dot{V}_D = 6.07\ 10^{-5}\ dm^3 s^{-1}$$
$$[\text{domain size}] = [-0.15 : 0.15] \text{ x } [-0.15 : 0.15] \text{ x } [0.0 : 1.2]\ dm^3$$
$$[\text{inner capillary radius}] = R_1 = 0.015\ dm \quad [\text{outer capillary radius}] = R_2 = 0.030\ dm$$
$$[\text{primary phase inflow radius}] = R_3 = 0.15\ dm.$$

The bounday conditions imposed on the inflow velocity are the following:

$$w = \begin{cases} a_2(R_1 - r)(R_1 + r) & \text{if} \quad 0 < r < R_1 \quad \text{(Dispersed phase)} \\ a_1(R_3 - r)(r - R_2) & \text{if} \quad R_2 < r < R_3 \quad \text{(Continuous phase)} \\ 0 & \text{otherwise,} \end{cases}$$

where the parameters a_1 and a_2 can be computed from the required volumetric flowrates.

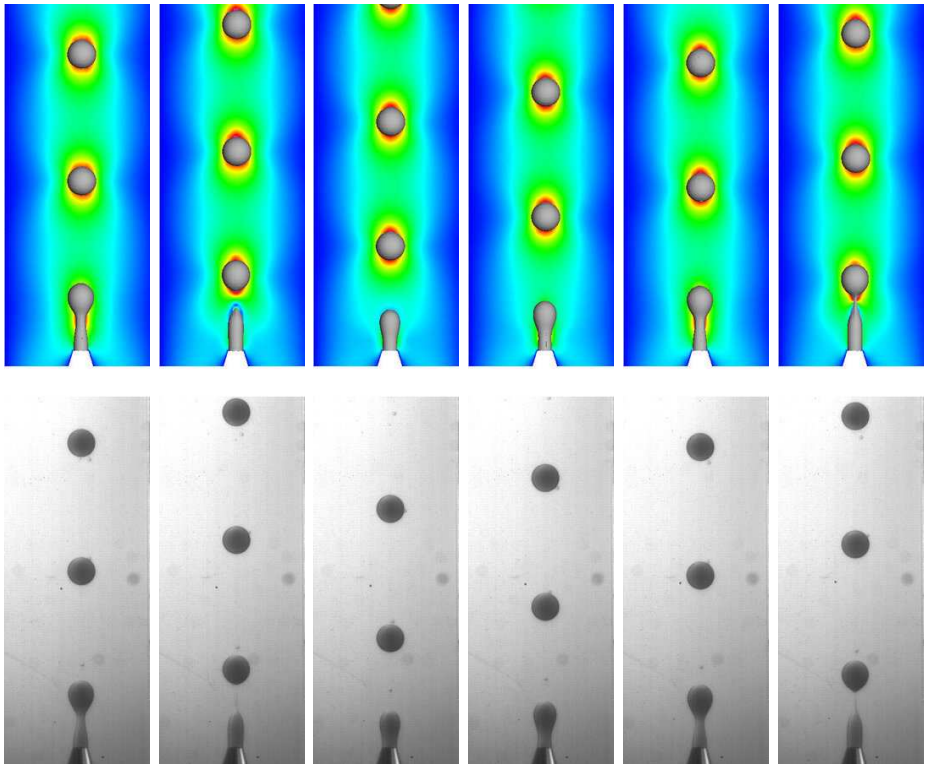

Figure 5: Sequence of one droplet separation compared with experimental measurement.

The resulting process leads to a pseudo-steady state, where the droplet separation happens according to the so called dripping mode. The frequency of the given mode is $f = 0.60\ Hz$ (cca $0.58\ Hz^{\text{exp}}$), which produces droplets of size $d = 0.058\ dm$ (cca $0.062\ dm^{\text{exp}}$). The maximum stream length during the process is $L = 0.102\ dm$ (cca $0.122\ dm^{\text{exp}}$). The snapshots of one full droplet generation compared with experimental measurements are given in the following figures (see Fig. 5).

4. CONCLUSIONS

In this contribution, we have shown that the realization of the newly redesigned high order FEM-Level Set approach supported by the subgrid surface reconstruction and octree based reinitialization mechanism provides a very robust framework for multiphase flow simulations with special emphasis on droplet generation from liquid jets. In parallel to that we have highlighted our recent development in the field on non-Newtonian multiphase flow on the example of two dimensional rising bubbles in viscoelastic fluids. Our future tasks are related to the combination of the two separate developments into one compact three dimensional simulation tool so to create a production CFD code being able to predict process parameters in achievement of the required quality of dispersed mixtures.

5. ACKNOWLEDGEMENTS

The authors like to thank the German Research foundation (DFG) for partially supporting the work under grants Sonderforschungsbereich SFB708 (TP B7), SFB TRR 30 (TP C3), SPP SPRAY 1423 (Tu102/32-1) and the group of Prof. Walzel at TU Dortmund for the experimental measurements supported by the grants Paketantrag PAK178 (Tu102/27-1, Ku1530/5-1).

References

[1] Clift R., Grace J. R., Weber M. E., *Bubbles, Drops and Particles.* Dover Publications, 2005, ISBN-13:978-0486445809.

[2] Damanik H., Hron J., Ouazzi A., Turek S., A monolithic FEM approach for the log-conformation reformulation (LCR) of viscoelastic flow problems, *Journal of Non-Newtonian Fluid Mechanics*, 2010, **165**(19-20):1105–1113, DOI: 10.1016/j.jnnfm.2010.05.008.

[3] Damanik H., Hron J., Ouazzi A., Turek S., Monolithic Newton-multigrid solution techniques for incompressible nonlinear flow models, *International Journal for Numerical Methods in Fluids*, 2012, DOI: 10.1002/fld.3656.

[4] Hysing S. *Numerical Simulation of Immiscible Fluids with FEM Level Set Techniques.* PhD Thesis, TU Dortmund, Institute of Applied Mathematics (LS III), Dortmund, 2007.

[5] Hysing, S., Turek, S., Kuzmin, D., Parolini, N., Burman, E., Ganesan, S., Tobiska, L., Quantitative benchmark computations of two-dimensional bubble dynamics. *International Journal for Numerical Methods in Fluids* 2009, **60**(11):1259–1288, DOI: 10.1002/fld.1934.

[6] Liu, Y. J., Liao, T. Y., Joseph, D. D. A two-dimensional cusp at the trailing edge of an air buble rising in a viscoelastic liquid, *Journal of Fluid Mechanics*, 1995, **304**:321–342.

[7] S. Turek, *Efficient Solvers for Incompressible Flow Problems: An Algorithmic and Computational Approach*, LNCSE 6, Springer, 1999.

[8] Turek S. On discrete projection methods for the incompressible Navier-Stokes equations: an algorithmical approach. *Computer Methods in Applied Mechanics and Engineering* 1997; **143**(3-4):271–288, DOI: 10.1016/S0045-7825(96)01155-3.

[9] S. Turek, O. Mierka, D. Kuzmin, and S. Hysing, Numerical study of a high order 3D FEM-Level Set approach for immiscible flow simulation, *Numerical methods for differential equations, optimization and technological problems.* Springer, 2012.